CHEMILUMINESCENCE SENSOR FOR 3D NOx CHARACTERIZATION IN LEAN-PREMIXED FLAME (LPP) COMBUSTION PROCESSES

Gustavo Lima Carneiro
Department of Mechanical Engineering, University of Brasilia
Campus Universitario Darcy Ribeiro, Brasilia, DF, Brazil
gugaunb@yahoo.com.br

Armando Caldeira-Pires
Department of Mechanical Engineering, University of Brasilia
Campus Universitario Darcy Ribeiro, Brasilia, DF, Brazil
armandcp@unb.br

Geovany Araújo Borges
Department of Electrical Engineering, University of Brasilia
Campus Universitario Darcy Ribeiro, Brasilia, DF, Brazil
gaborges@ene.unb.br

Abstract. *This paper describes an optics-based chemiluminescence sensor for NOx characterization of combustion process in turbine combustors. Lean premixed combustion is an important method for the reduction of NOx emissions from industrial turbine combustors. Lean fuelling has the overriding disadvantage that combustion induced oscillations arise and can destroy the machine. A chemiluminescent sensor is potentially able to measure these spatial and temporal variations, simultaneously verifying the origin of the combustion induced oscillations and assessing spatial and temporal inhomogeneity of the premixed mixture. The chemiluminescence sensor described in this paper measures flame geometric (area, locus of maximum intensity, center of mass) and light intensity (histogram, statistics moments) parameters of main intermediary reactants associated with chemical kinetics of prompt NOx production. In this context, CH chemiluminescence is assessed, and used to identify NOx emission intensity. The CH results are compared with NOx concentration based on gas analyzer measurements. Moreover, results of mean temperature and main chemical species concentration related with fuel and air flows are used to evaluate the capacity of this sensor to assess NOx production. In this context, the ability of the sensor to measure in a modified micro-turbine environment burning a LPG/air is demonstrated.*

Keywords*: LPP Combustion Chamber , NO measurement, Optical Sensor , Chemiluminescence*

1. Introduction

The objective of increasing combustor's performance, and, at the same time, reducing pollution's NO emissions in gas turbine combustors, has brought to the development of new combustion systems which use premixed flames (Barrag and Lawton, 1993, Baldini et al., 2000). A disadvantage of these systems is that premixed combustion are subjected to combustion instability (Baldini et al., 2000). This phenomenon is extremely dangerous for the combustor integrity, mainly due to pressure oscillations producing vibrations which can cause structural yielding and high level of acoustic noise.

The requirements on optimized operating conditions demand advanced combustion control systems, mainly associated with reduced pollutant levels restrictions. Although many different types of turbines combustors exist, in all of them combustion control are essentially performed through end-product of the combustion process, namely temperature, heat fluxes and combustion efficiency, since they are closely linked with production of pollutants, and energetic efficiency.

Therefore, the information necessary to control these complex processes is based on physical and electrochemical sensors measuring these variables. This information, however, is limited to overall characteristics in zones of easy access and do not allow the complete characterization of the combustion processes within the combustion chambers and the identification of non-conventional perturbations. On the other hand, the continuous improvement of the digital image analysis systems has fostered the use of visualization methods, which has allowed the implementation of novel control strategies for industrial combustion systems, including monitoring, maintenance and fault diagnosis. These imaging systems detect relevant information of the flame geometry and spectral emission range. Moreover, these new variables can be correlated with more orthodox data to provide important operational and performance trends (Oikawa, 1996, Lu et al, 1999).

This study was based on the assumption that there is a strong link between the control parameters and the flame characteristics (shape, intensity, and spectral distribution). On this regard, it was developed an experimental algorithm, based on off-line image processing, which computes main temporal behavior of geometric, light intensity and spectral distribution parameters of the flame, associated with mean results of NOx emission at the outlet of the combustor.

2. Methodology for images analysis

2.1. Experimental Installation and Chemiluminescence Image Acquisition

In this sense, a laboratory model of a Lean Premixed Prevaporized (LPP) combustion chamber was used to allow analysis of confined bluff-body stabilized premixed flames. This experimental rig was described in more details elsewhere (Caldeira-Pires et al., 2003), and basically it comprehended a premixing chamber and the combustion chamber. A bluff-body is positioned at the entrance of the combustion chamber to stabilize the flame. Figure 1 shows the Computational Fluid Dynamics (CFD) modeled image of the physical model used within this study.

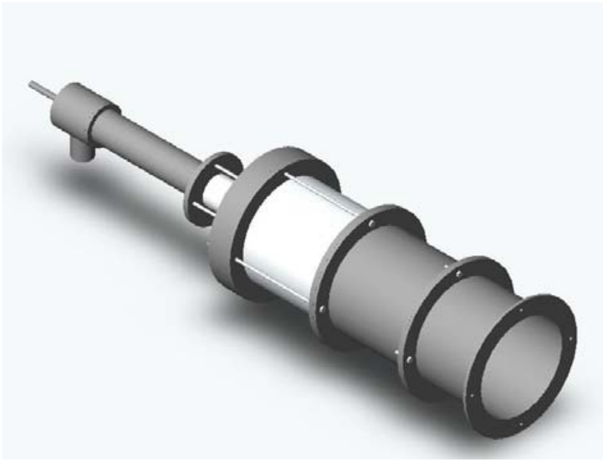

Figure 1. CFD-based virtual image of the LPP Laboratory Model
(including a cylindrical UV quartz combustion chamber)

In this experimental work, LPG (Liquified Petroleum Gas, mainly C_3 and C_4 hydrocarbon) is selected for fuel, mainly because is the easiest low molecular weight hydrocarbon commercially available. The fuel and the air were used in atmospheric conditions, accordingly the mass flow rates presented by Table 1.

A CCD 8-bit monochromatic camera is placed perpendicular to the UV-quartz section of the combustor, obtaining line-of-sight summed radial projections of the flame emission. The UV-quartz section has up to 60% transmittance at 220nm. The video output signals were connected to a frame grabber, and used for the acquisition of independent monochromatic video signals. Commercial 50mm UV lens (f = 1.4) allowed a cone collection of light of about 20^o, minimizing the distortion due to wide-angle imaging. Visible interference filter centered at 431nm±10nm for CH free radical imaging, with transmittance of 50%, is used for acquisition of monochromatic flame images. A dedicated software library was used in order to control the frame grabber (EPIX, 2002a, 2002b).

The flame images acquisition procedure consisted of obtaining time-averaged images encompassing the filter wavelength range, for a single projection, as the average flame characteristics are axi-symmetric. Figure 2 depicts the evolution of the Root Mean Square (RMS) of the pixel value difference between two consecutive averaged images. It can be verified that above 150 frames the resulting averaged image presented negligible differences.

Tomographic reconstruction software was built for this purpose, performing images ratio calculation as well, as reported by Caldeira-Pires (1999).

Table 1. Flow conditions range to be used during the experiments

Equivalence Ratio	Mass $Flow_{Fuel}.x10^{-3}$ (kg/s)	Mass $Flow_{Air}$ x 10^{-3} (kg/s)	Re $_{(calculated)}$
0,47	0,8935	29,415	31587
0,5	0,9505	29,415	31650
0,55	1,0455	29,415	31755
0,6	1,1405	29,415	31860
0,62	1,1785	29,415	31902
0,7	1,3306	29,415	32070

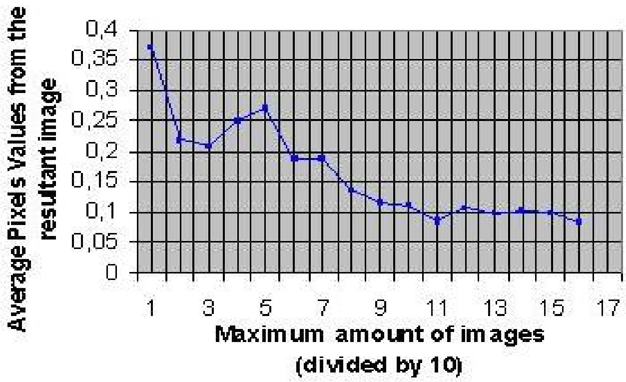

Figure 2: Pixels values variation versus average images pairs.

2.1. Identification of flame features

The imaging system studied aimed at providing information considered useful to identify within a set of several flames conditions, namely by processing each digitized flame image. Therefore, it involves a low level image processing step and some specific data to be extracted from each image. On this regard, an attempt was made to establish a set of useful information that could be used to describe each flame image, which meant the combustion conditions, performance and pollutant emissions.

The methodology implemented encompassed four main steps: the identification of areas of interest (AOI), the tomographic reconstruction of the volumetric emission locus, the calculation of geometrical parameters and characterization of histogram profile. As far as geometrical parameters were concerned, flame area and locus of maximum intensity (which measures the flame separation from the bluff body) were defined as main characteristics to be analyzed (Costeiro and Santieiro, 1991, Baldini et al., 2000). Other features associated with flame brightness were characterized by the analysis of the histogram and the statistics Reynolds moment.

The extraction of these numerical parameters from the images were performed after the tomographic reconstruction algorithm, therefore these variables characterized the real source of emissions within the flame, since the tomographic images represent the radial emission and not the summation of emissions across the whole optical path from the flame to the camera.

On this regard, Figure 3 displays the tomographically reconstructed emission region and the mean projection as acquired by the imaging system. These two figures depict the differences between a projection, which represents the summation of all the radiation being emitted along the line-of-sight of each pixel, and its reconstructed image, showing the radial profile (*tomos*, or slice) of emission region within the flame.

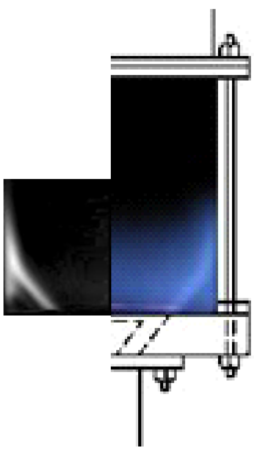

(a) **(b)**

Figure 3: Reconstructed Image and Mean Projection of Chemiluminescence emission:
(a) Free Radical Chemiluminescence Reconstructed Image,
(b) CH Free Radical Chemiluminescence Projection

2.3. Histogram-related parameters

The profile of the histogram for each flame condition was calculated by means of Reynolds statistics analysis. In this context, it was calculated the mean value, variance, rms, skewness and flatness, translating the histogram shape into numerically accessible parameters to be assessed (on image processing, see also Gonzalez and Wintz, 1987, and Rabbani, 1995).

2.4. Diagnostics Intrusive Techniques

In the same time, informations related to the temperature of the flame was acquired, through termocouple (R type) and measurements about the concentration of the gases (O_2, NO, CO, C_xH_y) were obtained as well, in the end of the combustion chamber, by a gas analyser. The flow conditions of the reagents fuel+air did not change, therefore the velocity components of the mixture were kept constant.

The following data were acquired and, parallel to that process, the images of the flame were obtained:

- Temperature (in the end of the LPP chamber): it was made a lot of measures of the temperature along the chamber diameter. An average value would then reflect the temperature of the flame;
- Air flow;
- Fuel flow (LPG);
- Chemical species concentration: CO_2, CO (ppm and percentual), NO and CH.

3. Results

The flame images obtained from several equivalence ratio Φ - which is defined as the quotient between the ratio $(F/A)_{mixture}$ and $(F/A)_{stoichiometric}$, where F is the mass of fuel and A is the mass of air injected (in a time interval) – are shown in Figure 4.

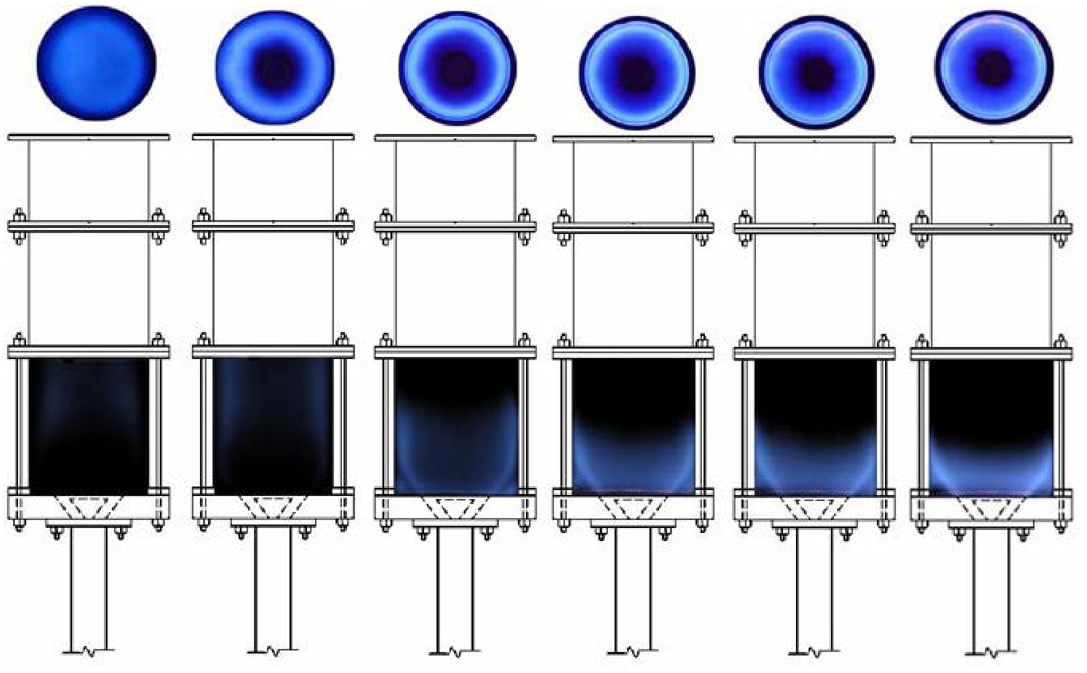

Φ = 0.47	**Φ = 0.50**	**Φ = 0.55**	**Φ = 0.60**	**Φ = 0.62**	**Φ = 0.70**

Figure 4. Flame projections for each equivalence ratio Φ

It was necessary to make the tomographic reconstruction of the image from the flames, intending to get the central profile of it. This is necessary because the images obtained are the sum of an optical path, instead of the image of the flame in the center of the chamber. A program written in MatLab code was used to achieve the tomographic reconstruction. It was taken into account that there was axial symmetry in the obtained flame images. The results after the reconstruction are shown in Figure 5, for each equivalence ratio Φ.

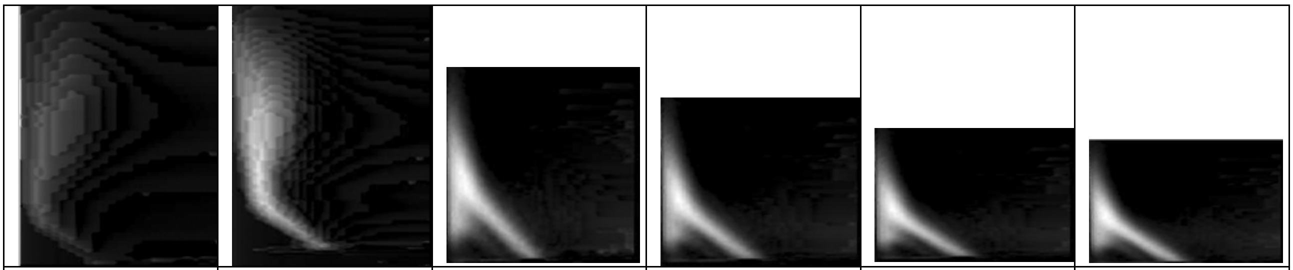

Figure 5: Flame reconstructed images for each equivalence ratio Φ

It is important to emphasize that, in the images of Figure 5, what is seen is just the light spectrum related to the wavelength of the radiation proceeding from CH radical. It has been made possible through filters used in the CCD camera, specific for the mentioned radiation.

The main characteristics to be identified in each image are the white cloud at one of the side of the picture, which is the brighter (hottest) and most significant part of the flame regarding the NOx production. The technique made use of edge detection techniques to identify flame limits and afterwards calculate its geometric parameters.

The data obtained in this research are shown in Tables 2 and 3 and Figures 6 to 8. Namely, Table 2 presents the gas analysis results and Table 3 depicts Reynolds moments for the pixel intensity value statistics and geometric parameters of the flame zone of each equivalence ratio.

Table 2: Data from the chemical species obtained in the end of the Combustion Chamber LPP.

Φ	Temp. °C	% O2	%CO2	CO ppm	CO%	NO ppm	NOx ppm	CxHy %
0.47	939,	11,7	6,47	637,4	0,065	6,08	6,67	0,078
0.50	993,	11,0	6,64	3,9786	0,00143	6,07	6,21	0,020
0.55	1014,	9,94	7,76	0	0	7,93	7,93	0,023
0.60	1036,	9,06	7,87	0	0	8,13	8,40	0,025
0.62	1048,	8,71	8,03	0	0	8,27	8,33	0,033
0.70	1066,	8,21	8,48	0	0	8,60	8,73	0,033

Table 3: Data accomplished by the image processing.

Φ	Mean	Variance	rms	Skewness	Flatness	Distance to Burner (N^o. Pixels)	Area (%)
0.47	21.061	264.68	16.269	0.508	2.653	245.030	72.3
0.50	22.468	900.79	30.013	3.095	17.36	289.904	59.1
0.55	33.490	2629.2	51.275	2.092	6.672	338.268	56.9
0.60	30.913	2607.4	51.062	2.273	7.441	358.121	53.2
0.62	30.248	2697.4	51.936	2.340	7.752	364.493	51.5
0.70	27.249	2425.4	49.247	2.442	8.358	367.418	47.1

Figure 6 displays the evolution of the results of image analysis, as presented by Table 3, with the equivalence ratio. The increase of the equivalence ratio increases flame temperature and NOx concentration as well, but decreases the flame area.

Figure 7 shows the histograms of each equivalence ratio average projection, presenting the evolution of the amount of pixels at each gray level of a 8-bit monochromatic image (256 levels). This series of graphics shows that increasing Φ augments the intensity of the flame, which can be depicted by the distribution over a higher range of gray levels.

At least Figure 8 shows that decreasing Φ the brighter pixel moves downward into the flow. The projections are inverted, in the sense that the higher intensity is black and vice-versa. This increase of the distance to the burner is associated with a narrow range of gray levels, as presented by Figure 7.

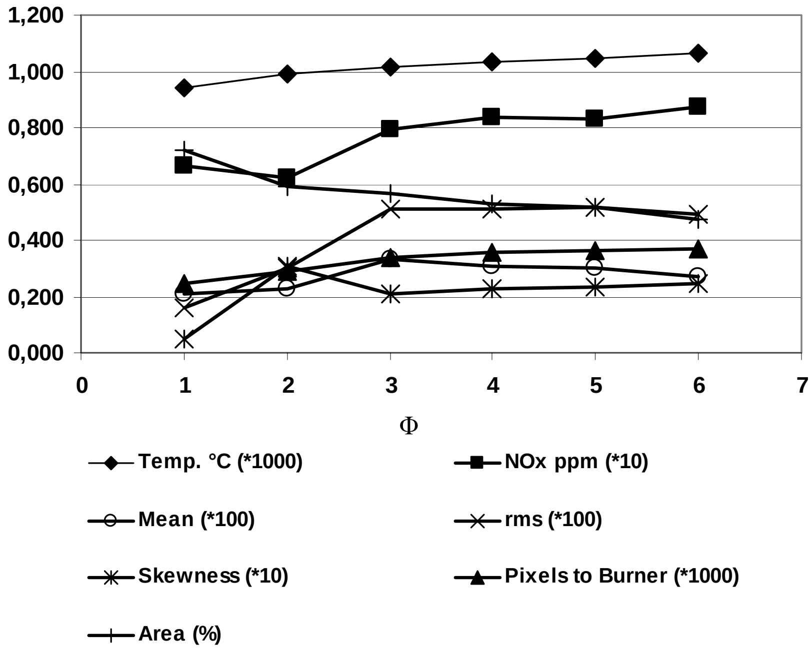

Figure 6: Evolution of Tables 2 and 3 main parameters with Equivalence Ratio, Φ (1 – 0.47; 2 – 0.50; 3 – 0.55; 4 – 0.60; 5 – 0.62; 6 – 0.70)

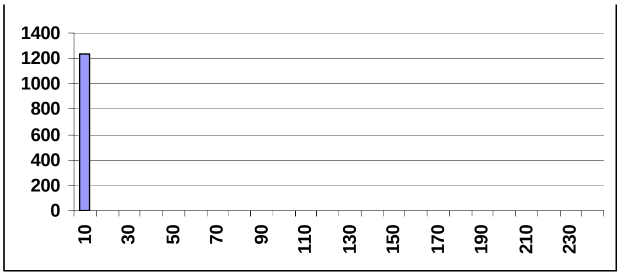

Φ = 0,47

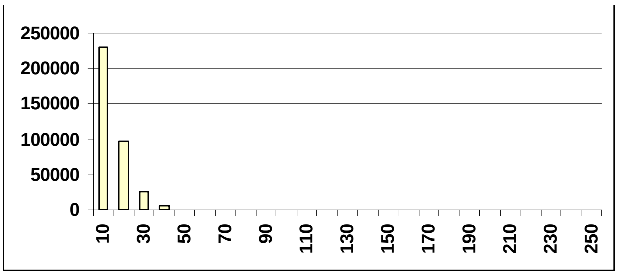

Φ = 0,5

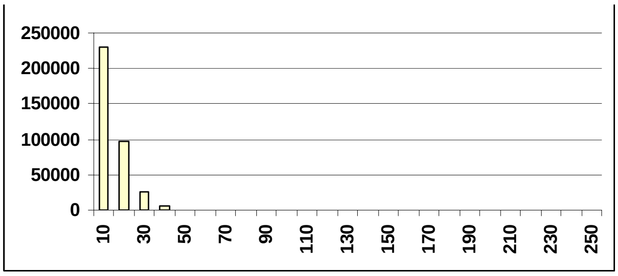

Φ = 0,55

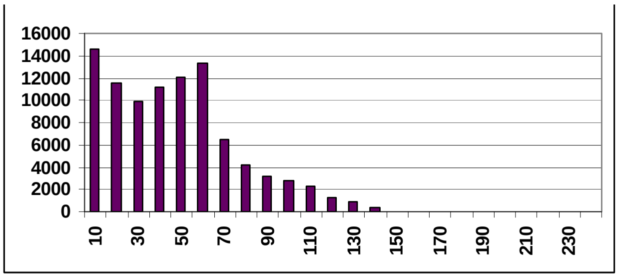

Φ = 0,6

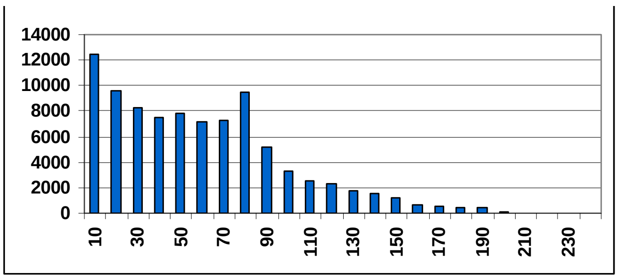

Φ = 0,62

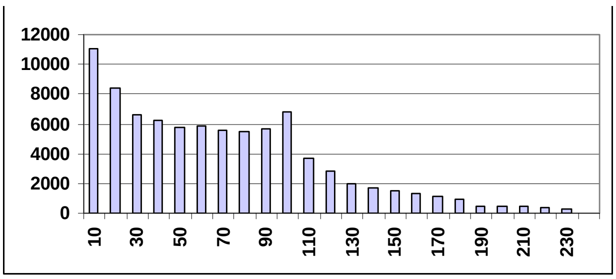

Φ = 0,7

Figure 7: Histograms describing the distribution of the pixel values for each equivalence ratio Φ over the 256 gray levels of a 8-bit image.

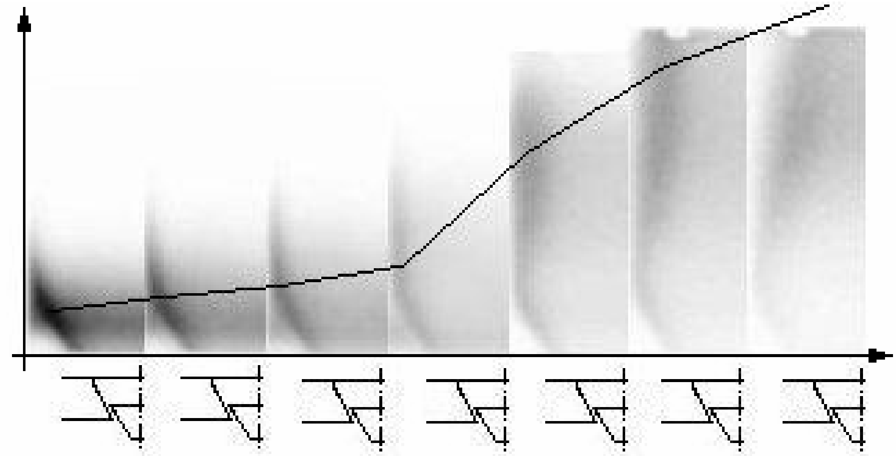

0,7	0,62	0,6	0,55	0,52	0,50	0,47

Figure 8: Reconstructed images and the evolution of the point of maximum intensity with the equivalence ratio

According to the obtained data, it can be seen clearly that there is an increase in the amount of the chemical specie NO as the temperature goes up (Table 2). It was a predicable result, as the heating is related to the emission of that pollutant.

The analysis of the CH chemiluminescence brought some important relations that can be correlated to the NO emission:

1) An increase tendency in the light intensity of the images was observed, reflecting the increase of the average pixel values, as the equivalent ratio Φ was also carried up, when fuel was injected in a bigger amount with air. The measurement of the quantity of NO revealed it was increasing with the equivalence ratio Φ. Then, an increase in the production of CH radical (inferred from the stronger luminosity of the flame) leads to an increase in the production of NO.
2) Other important information to be considered relates a geometric characteristic of the flame (its area) with the emission of NO. An increase in the equivalence ratio resulted always in a reduction of the area calculated for the flame. It was considered that, to be part of the flame, the pixel value should have a minimum (threshold), which was considered to be 10, that means 3% of the value of the maximum intensity the CCD device was able to acquire (8 bits/pixel yields 255 as the higher value). It was considered to be a reasonable value that ensures us to really deal the flame image. Therefore, the reduction of the area of the central profile of the flame is related to an increase of the emission of NO radical.
3) Considering that the center of mass of the flame contour can be calculated, it was observed it moved away from the center of the burner, as the equivalence ratio increased. That was not the expected behavior for values of that parameter, as the flame became reduced while the fuel injection was increased, concentrating itself closer to the burner, and, therefore, its center of mass should indicate an approach to that element.
4) Another important parameter to be taken into account would be the maximum values of the pixels, indicating the maximum intensity of the flame. However, for a equivalence ratio higher than 0.52, the values of the pixels saturated, which means they reached the maximum possible value, and therefore nothing could be inferred, about the relation between that parameter of the flame and the emission of the pollutant NO.
5) The image histograms showed that the higher equivalence ratio, more abrupt is the distribution among the smallest values reached by the pixels and those ones taken as the cloudy deep, which don't correspond to the flame. In fact, as the area of the flame diminished, however, in general, they became more intense in its luminosity, reflecting the accented changes in the images histograms.

It must be pointed out that the measurements of other chemical compounds in the end of the chamber brought further information related to the diagnosis of NO emission. For example, an increase in the C_xH_y (hydrocarbon) results, in general, in a bigger amount of NO emitted. Nevertheless, the accuracy of the chemical measurement device (gas analyzer) is quite near to the measured values, and then, a rigorous analysis that relates the emission of some chemical radicals to the NO emission, during the burning, stays compromised. However, the research points out a correlation between the visual information obtained from the CH radical and the NO emission. More visual evidences must be found out, in order to confirm the link between them.

4. Conclusions

This research demonstrated that there is a relation between the NO production and free radical CH emission, pointed through the analysis of that hydrocarbon images. Since the visual detection of radical is technologically able to be performed, it indicates a direction for a conception of new NO emission sensor, based entirely on the observation of CH emission, considered like a reasonable indicative to be studied.

With the information obtained, there will be the generation of a data base that will assign the combustion process and its parameters with the “visual signature” of the flame, making viable the development of the chemiluminescence sensor, and it will be possible to identify the generation of the pollutant based on the visual information of the flame. Therefore, extracting the images from the pollutants is possible to identify which flow conditions and equivalence ratio are linked to the emission of the chemical radicals (*e.g,* CH and C_2), and the identification of NO_X production will be possible. This kind of identification can be used by a system of control of the combustion process intended to decrease the pollutants emission, as a result of hydrocarbon fuel combustion processes.

5. Acknowledgments

Financial support has been provided by the Eletronorte Research and Development Funding Program, in the context of the Electrical Energy Sector Fund, under the contract nº Eletronorte 4500013171, and by CNPq, in the context of the PROFIX program, nº 540580/01-5, and the PIBIC 2004 program.

6. References

Baldini, G., Campadelli, P., Lanzarotti, R., 2000, “Combustion analysis by image processing of premixed flames”, Proceedings. 2000 IEEE-International Conference on Image Processing, Volume 2, 10-13 Sept. 2000 Page(s):708 - 711 vol.2, pp.708-711.

Barrag, A., Lawton, B, 1993, “Computer optical tomography in the study of internal combustion engine soot concentration”, Proceedings of 26th International Symposium on Automotive Technology and Automation, Vol.: The motor vehicle and the environment – demands of the nineties and beyond, September 1993, Aachen.

Caldeira-Pires, A., Correia, D.P. , Ferrão, P., Heitor, M.V. “Temperature tomographic sensor for combustion analysis”, Instituto Superior Técnico de Lisboa.

Costeira, J. V. Sentieiro, J., 1991, “A computer vision system for the characterization and classification of flames in glass furnaces”, Instituto Superior Técnico, Lisbon.

EPIX, 2002a, “Reference Manual - XCLIB C Library Version 2.2”, EPIX - Image Processing Products For Research and Industry Inc., Illinois, USA.

EPIX, 2002b, “Reference Manual - PXIPL Image Processing C Library for XCLIB V2.2”, EPIX - Image Processing Products For Research and Industry Inc., Illinois, USA.

Gonzalez, R. C., Wintz, P, 1987, “Digital Image Processing”, 2nd Edition, Addison-Wesley Publishing Company, Canadá.

Lu, G., Yan, Y., and Ward, D.D., 2000,“Advanced, monitoring, characterization and evaluation of gas-fired flames in a utility boiler”, J. of the Institute of Energy, 73, pp. 43-49.

Oikawa, T., Tomizawa, M., Degawa, S., 1996, “New Monitoring System for Thermal Power Plants Using Digital Image Processing and Sound Analysis”, Control Eng. Practice, Vol.5, N° 1, pp 75-78.

Rabbani, M., 1995, “Introduction to Electronic Imaging”, Eastman Kodak Research Labs, SPIE – The International Society for Optical Engineering.

7. Responsibility notice

The authors are the only responsible for the printed material included in this paper.